Development and Validation of a Wear Model for the Prediction of Wheel and Rail Profile Evolution on Complex Railway Networks

Mirko Ignesti [1], Alice Innocenti [1], Lorenzo Marini [1], Enrico Meli [1], Andrea Rindi [1]

[1] Department of Industrial Engineering, University of Florence, via Santa Marta 3, Florence, Italy:
mirko.ignesti@unifi.it, alice.innocenti@unifi.it, lorenzo.marini@unifi.it, enrico.meli@unifi.it, andrea.rindi@unifi.it

Abstract

In railway applications, the wear estimation at the wheel-rail contact is an important field of study, mainly correlated to the planning of maintenance interventions, vehicle stability and the possibility to carry out specific strategies for the wheel profile optimization. In this work the Authors present a model for the evaluation of the wheel and rail profile evolution due to wear specially developed for complex railway networks. The model layout is made up of two mutually interactive but separate units: a vehicle model for the dynamical analysis and a model for the wear evaluation.To study complex railway lines the Authors also proposed a new statistical approach for the railway track description in order to achieve general significant accuracy results in a reasonable time. The wear model has been validated in collaboration with Trenitalia S.P.A and Rete Ferroviaria Italiana (RFI), which have provided the technical documentation and the experimental data relating to some tests performed on a scenery that exhibits serious problems in terms of wear: the vehicle *DMU ALn 501 Minuetto* circulating on the Aosta-Pre Saint Didier Italian line.

Keywords: *Wheel-rail wear, Multibody modeling of railway vehicles, Statistical track analysis*

1 Introduction

In this work the Authors present a procedure to estimate the evolution of the wheel and rail profiles due to wear specifically developed for complex railway networks. In literature many important research works regarding the wear estimation can be found [1][2]. However a substantial lack is present in the literature concerning wear models specially developed for complex railway network applications. In this case the computational load needed to carry out the exhaustive simulation of vehicle dynamics and wear evaluation turns out to be absolutely too high for each practical purpose. To overcome this critical issue of the wear prediction models, the Authors propose a new track statistical approach to reach relevant results in a reasonable time; more specifically the Authors suggest to replace the entire railway network with a discrete set of N_c different curved tracks (classified by radius, superelevation and traveling speed) statistically equivalent to the original network. The new approach allows a substantial reduction of the computational load and, at the same time, assures a good compromise in terms of model accuracy. This work has been carried out in collaboration with Trenitalia S.p.A. and RFI that have provided the experimental data concerning the Aosta-Pre Saint Didier railway line and the vehicle ALSTOM *DMU Aln 501 Minuetto* needed for the preliminary model validation.

2 General Architecture of the Model

The general architecture of the model developed for studying the wear phenomena on complex railway lines is made up of two main parts: the *vehicle model* necessary to perform the dynamical analysis and the *wear model* (see Fig. 1). The *vehicle model* (realized in Simpack Rail environment) consists of the multibody model of the benchmark railway vehicle and the 3D global contact model that, during the dynamical simulation, interact directly online creating a loop. At each time integration step the first one evaluates the kinematic variables (position, orientation and their derivatives) relative to the wheelsets and consequently to each wheel - rail contact pair and the second one, starting from the kinematic quantities, calculates the global contact variables (contact points and contact forces, contact areas and global creepages) [3][4]. The main inputs of the *vehicle model* are the multibody model of the railway vehicle and the corresponding railway track, represented in this work by the ALSTOM *DMU Aln 501 Minuetto* and the Aosta-Pre Saint Didier line respectively. In the wear estimation research activities the track description is a critical task due to the complexity of the railway networks to be studied: to overcome these limitations, a new statistical approach has been developed to achieve general significant results in a reasonable time. In particular the entire considered railway network has been replaced with a discrete set

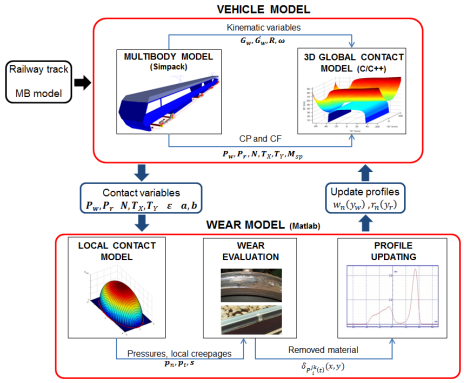

Figure 1: General architecture of the model.

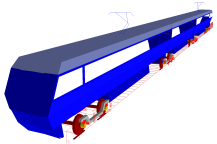

Figure 2: Global view of the multibody model.

Table 1: Inertia properties of the multibody model.

MBS body	Mass kg	Roll Inertia kgm^2	Pitch Inertia kgm^2	Yaw Inertia kgm^2
Coach (motor)	31568	66700	764000	743000
Coach (trailer)	14496	30600	245000	236000
Bogie (motor)	3306	1578	2772	4200
Bogie (trailer)	3122	1674	3453	5011
Wheelset (motor)	2091	1073	120	1073
Wheelset (trailer)	1462	1027	120	1027

of N_c different curved tracks (classified by radius, superelevation and traveling speed) statistically equivalent to the original network. The *wear model* (fully implemented in Matlab environment) is the part of the procedure concerning the prediction of the amount of worn material to be removed from the wheel and rail surfaces and is made up of three distinct phases: the local contact model, the wear evaluation and the profile update. The local contact model, starting from the global contact variables, estimates the local contact pressures and creepages inside the contact patch and detects the creep zone of the contact area [4]. Subsequently the distribution of removed material is calculated both on the wheel and on the rail surface only within the creep area by using an experimental relationship between the removal material and the energy dissipated by friction at the contact interface [1]. Finally the wheel and rail worn profiles are derived from the original ones through an appropriate innovative update strategy. The new updated wheel and rail profiles (one mean profile both for all the wheels of the vehicle and for all the rails of the considered tracks) are then fed back as inputs to the *vehicle model* and the whole model architecture can proceed with the next discrete step. The evolution of the wheel and rail profiles is therefore a discrete process. The choice of the discrete step for the profiles updates as it will be clarified in the following, has to consider the difference between the time scales characterizing the wheel and rail wear evolution rates.

3 The Vehicle Model

The benchmark vehicle investigated for this research is the *DMU Aln 501 Minuetto*, a passenger transport unit widespread in Italian Railways where is equipped with the standard ORE S1002 wheel profile and UIC60 rail profile canted at $1/20$ rad. This particular vehicle exhibits in fact severe wear and stability problems mainly caused by the adopted matching. Its mechanical structure and its inertial, elastic and damping properties can be found in literature [5][6]. In Tab. 1 the inertia properties of the vehicle are shown by way of example. The multibody model (see Fig. 2) consists of thirty-one rigid bodies: three coaches, four bogie (the intermediate ones, interposed between two successive coaches, are trailer bogies while the other ones are motor bogies), eight wheelsets and sixteen axleboxes. The rigid bodies are connected by means of appropriate elastic and damping elements; particularly the vehicle is equipped with two suspension stages. Both the stages of suspensions have been modeled by means of three-dimensional viscoelastic force elements taking into account all the mechanical non linearities of the system (bumpstop clearance, dampers and rod behaviour). In this research activity a specifically developed 3D global contact model has been used in order to improve reliability and accuracy of the contact points detection. In particular the adopted contact model is based on a two step procedure; the contact points detection [3, 7] and the global contact forces evaluation [4]. The contact points detection algorithm is based on a classical formulation of the contact problem in multibody field and the most innovative aspect of the proposed method is the reduction of the algebraic problem dimension (from 4D to a simple 1D scalar problem) through exact analytical procedures. Finally, for each detected contact point, the global creepages ε_x, ε_y, ε_{sp} in the contact patch and the normal N^r and tangential T_x^r, T_y^r contact forces are determined [4].

4 The Wear Model

4.1 The Local Contact Model

The inputs of the wear model are the global contact parameters estimated by the vehicle model. Since a local wear computation is required, the global contact parameters need to be post-processed and this can be achieved through the

simplified Kalker's theory implemented in the FASTSIM algorithm. This theory starts from the global creepages (ε_x, ε_y, ε_{sp}), the normal and tangential global forces (N^r, T^r_x, T^r_y), the contact patch dimensions (a, b) and the material properties to compute the local distribution of normal p_n and tangential $\mathbf{p}_t$ stresses and local creepages $\mathbf{s}$ across the wheel-rail contact area. For a more detailed description of the FASTSIM algorithm one can refer to the literature [4].

4.2 The Wear Evaluation

To evaluate the specific volume of removed material on wheel and rail due to wear $\delta_{P^j_{wi}(t)}(x,y)$ and $\delta_{P^j_{ri}(t)}(x,y)$ (where x and y indicate the coordinates of a generic point of the contact patch) related to the i-th contact points $P^j_{wi}(t)$ and $P^j_{ri}(t)$ on the j-th wheel and rail pair for unit of distance traveled by the vehicle (expressed in m), and for unit of surface (expressed in mm), an experimental relationship between the volume of removed material and the frictional work [1] has been used. More specifically, the local contact stresses $\mathbf{p}_t$ and creepages $\mathbf{s}$ are used to evaluate the *wear index* I_W (expressed in N/mm^2), which represents the frictional power generated by the tangential contact pressures: $I_W = \mathbf{p}_t \bullet \mathbf{s}/V$ where V is the longitudinal velocity speed. This index can be correlated with the *wear rate* K_W, that is the mass of removed material (expressed in μg/m mm^2) for unit of distance traveled by the vehicle and for unit of surface. The correlation is based on real data available in literature [1], which have been acquired from experimental wear tests carried out in the case of metal to metal contact with dry surfaces using a twin disc test arrangement. The experimental relationship between K_W and I_W adopted for the wear model described in this work is the following (Fig. 3):

$$K_W(I_W) = \begin{cases} 5.3 * I_W & I_W < 10.4 \\ 55.1 & 10.4 \leq I_W \leq 77.2 \\ 61.9 * I_W - 4778.7 & I_W > 77.2. \end{cases} \quad (1)$$

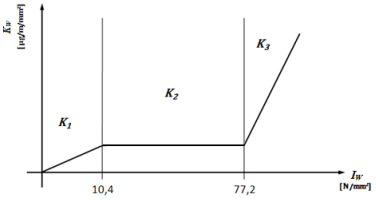

Figure 3: Trend of the *wear rate* K_W.

Once the wear rate $K_W(I_W)$ is known (the same both for the wheel and for the rail), the specific volume of removed material on the wheel and on the rail (for unit of distance traveled by the vehicle and for unit of surface) can be calculated (expressed in mm^3/m mm^2): $\delta_{P^j_{wi}(t)}(x,y) = K_W(I_W)\frac{1}{\rho}$, $\delta_{P^j_{ri}(t)}(x,y) = K_W(I_W)\frac{1}{\rho}$ where ρ is the material density.

4.3 The Profile Update Procedure

After obtaining the amount of worn material, wheel and rail profiles need to be updated to be used as the input of the next step of the whole model. The new profiles, denoted by $w_n(y_w)$ and $r_n(y_r)$, are computed from the old ones $w_o(y_w)$, $r_o(y_r)$ and from all the calculated distributions $\delta_{P^j_{wi}(t)}(x,y)$ and $\delta_{P^j_{ri}(t)}(x,y)$ of worn material through an appropriate set of numerical procedures that defines the update strategy (further details can be found in literature [7]). First of all the integration of the worn material on the wheel circumference length and on the track length provides the mean value of removed material in longitudinal direction $\delta^{tot}_{P^j_{wi}(t)}(y)$, $\delta^{tot}_{P^j_{ri}(t)}(y)$. Subsequently a track integration sums all the wear contributes of the dynamic simulation to obtain the depth of removed material for wheel and rail expressed in mm: $\Delta_{P^j_{wi}}(s_w)$, $\Delta_{P^j_{ri}}(s_r)$ (the introduction of the natural abscissas s_w and s_r of the curves $w(y_w)$ and $r(y_r)$ leads to a better accuracy in the calculation of the worn profiles). Then the sum on the contact points and the average on the wheel-rail pairs allows the evaluation of the average wear quantities $\overline{\Delta}^w(s_w)$, $\overline{\Delta}^r(s_r)$ needed to obtain as output of the wear model a single mean profile both for the wheel and for the rail.

At this point an average on the curved tracks is necessary when a statistical description of the track is adopted. In this case, different wear distributions $\overline{\Delta}^w_k(s_w)$ and $\overline{\Delta}^r_k(s_r)$ for each of the N_c curve classes will be obtained from the previous steps (with $1 \leq k \leq N_c$). The statistical weigths of the curve classes p_k (see paragraph 5.2), calculated as the ratio between the track length characterized by the curve conditions related to the k-th class (in terms of radius and superelevation values) and the total railway track length, have to be introduced to consider the frequency with which each curve appears on the actual railway track. Consequently, for the statistical approach, the following ralations for the removed material hold: $\sum_{k=1}^{N_c} p_k \overline{\Delta}^w_k(s_w) = \overline{\Delta}^w_{stat}(s_w)$, $\sum_{k=1}^{N_c} p_k \overline{\Delta}^r_k(s_r) = \overline{\Delta}^r_{stat}(s_r)$ with $\sum_{k=1}^{N_C} p_k = 1$. Obviously, when the dynamic simulations are performed on the complete railway track the previous equations simply become $\overline{\Delta}^w(s_w) = \overline{\Delta}^w_{track}(s_w)$, $\overline{\Delta}^r(s_r) = \overline{\Delta}^r_{track}(s_r)$.

Since it normally takes traveled distance of thousands kilometers in order to obtain measurable wear effects, an appropriate scaling procedure is necessary to reduce the simulated track length with a consequent limitation of the computational

effort. Hypothesizing the almost linearity of the wear model with the traveled distance inside the discrete steps, it is possible to amplify the removed material during the dynamic simulations by means of a scaling factor which increases the distance traveled by the vehicle. In this work adaptive discrete steps (function of the wear rate and obtained imposing the threshold values D^w_{step} and D^r_{step} on the maximum of the removed material quantity on the wheelsets and on the tracks at each discrete step) have been chosen to update the wheel and rail profiles (see eq. 2). The evaluation of the discrete steps for the profile updates, with the consequent scaling of $\overline{\Delta}^w_{stat}(s_w)$, $\overline{\Delta}^w_{track}(s_w)$ and $\overline{\Delta}^r_{stat}(s_r)$, $\overline{\Delta}^r_{track}(s_r)$, represents the major difference between the update strategy of wheel and rail:
1) the removed material on the wheel due to wear is proportional to the distance traveled by the vehicle; in fact a point of the wheel is frequently in contact with the rail in a number of times proportional to the distance. If km_{tot} is the total mileage traveled by the considered vehicle, km_{step} is the length of the discrete step corresponding to the threshold value on the wear depth D^w_{step} and km_{prove} is the overall mileage traveled by the vehicle during the dynamic simulations, the material removed on the wheels and the corresponding km_{step} value have to be scaled according to the following laws:

$$\overline{\Delta}^w_{stat}(s_w)\frac{D^w_{step}}{D^w_{stat}} = \overline{\Delta}^{w\ sc}_{stat}(s_w), \quad km^{stat}_{step} = \frac{D^w_{step}}{D^w_{stat}} km^{stat}_{prove}, \quad D^w_{stat} = \max_{s_w} \overline{\Delta}^w_{stat}(s_w); \tag{2}$$

$$\overline{\Delta}^w_{track}(s_w)\frac{D^w_{step}}{D^w_{track}} = \overline{\Delta}^{w\ sc}_{track}(s_w), \quad km^{track}_{step} = \frac{D^w_{step}}{D^w_{track}} km^{track}_{prove}, \quad D^w_{track} = \max_{s_w} \overline{\Delta}^w_{track}(s_w). \tag{3}$$

The km_{prove} parameter assumes a different value according to the different way in which the track is treated: if the wear evolution is evaluated on the overall railway track (of length l_{track}) then $km^{track}_{prove} = l_{track}$ while, if the track statistical approach is considered, $km^{stat}_{prove} = l_{ct}$ is the mileage traveled by the vehicle during each of the N_c dynamic simulations. This consideration explains the deeply difference in terms of computational load between the two considered cases.
2) the depth of rail wear is not proportional to the distance traveled by the vehicle; in fact the rail tends to wear out only in the zone where it is crossed by the vehicle and, increasing the traveled distance, the depth of removed material remains the same. On the other hand the rail wear is proportional to the total tonnage M_{tot} burden on the rail and thus to the total vehicle number N_{tot} moving on the track. Therefore, if N_{step} is the vehicle number moving on the track in a discrete step, the quantity of rail removed material at each step will be:

$$\overline{\Delta}^r_{stat}(s_r)\frac{D^r_{step}}{D^r_{stat}} = \overline{\Delta}^{r\ sc}_{stat}(s_r), \quad N^{stat}_{step} = \frac{D^r_{step}}{D^r_{stat}} N^{stat}_{prove}, \quad D^r_{stat} = \max_{s_r} \overline{\Delta}^r_{stat}(s_r); \tag{4}$$

$$\overline{\Delta}^r_{track}(s_r)\frac{D^r_{step}}{D^r_{track}} = \overline{\Delta}^{r\ sc}_{track}(s_r), \quad N^{track}_{step} = \frac{D^r_{step}}{D^r_{track}} N^{track}_{prove}, \quad D^r_{track} = \max_{s_r} \overline{\Delta}^r_{track}(s_r). \tag{5}$$

where $N^{stat}_{prove} = N_c$ and obviously $N^{track}_{prove} = 1$.

Then an appropriate smoothing of the worn material distributions is required to avoid the numerical noise and the short spatial wavelengths without physical meaning that affect the worn material distributions and could be passed to the new profiles $\tilde{w}^{stat}_n(s_w)$, $\tilde{w}^{track}_n(s_w)$ and $\tilde{r}^{stat}_n(s_r)$, $\tilde{r}^{track}_n(s_r)$ with consequent problems raising in the global contact model. Finally the update of the old profiles $\tilde{w}^{stat}_o(s) = w^{stat}_o(y)$, $\tilde{w}^{track}_o(s) = w^{track}_o(y)$ and $\tilde{r}^{stat}_o(s_r) = r^{stat}_o(y_r)$, $\tilde{r}^{track}_o(s_r) = r^{track}_o(y_r)$ to obtain the new profiles $\tilde{w}^{stat}_n(s) = w^{stat}_n(y)$, $\tilde{w}^{track}_n(s) = w^{track}_n(y)$ and $\tilde{r}^{stat}_n(s_r) = r^{stat}_n(y_r)$, $\tilde{r}^{track}_n(s_r) = r^{track}_n(y_r)$ is performed removing the worn material $\overline{\Delta}^{w\ \ sc}_{track\,sm}(s_w)$, $\overline{\Delta}^{r\ \ sc}_{track\,sm}(s_r)$ in the normal direction to the wheel and rail profile respectively.

5 Railway Track Description

5.1 The Aosta Pre-Saint Didier Line

The whole Aosta-Pre Saint Didier railway network (characterized by an approximate length of $l_{track} \approx 31$km) has been reconstructed and modeled in the Simpack environment starting from the track data provided by RFI. This is a very sharp track on the Italian Railways and the scenery is rather interesting since the *DMU Aln 501 Minuetto* exhibits serious problems on this track in terms of wear, requiring frequent maintenance interventions on the wheelsets.

5.1.1 Wear Control Parameters and Experimental Data

The reference parameters FH (flange height), FT (flange thickness) and QR quota are capable of estimating the wheel profile evolution due to wear without necessarily knowing the whole profile shape (see Fig. 4) [8]. An additional control parameter is then introduced to evaluate the evolution of rail wear. Particularly the QM quota is defined as the rail head height in the point $y_r = 760\ mm$ with respect to the center line of the track (see Fig. 5).

The experimental data provided by Trenitalia have been measured for all the vehicle wheels on three different vehicles *DMU Aln 501 Minuetto* operating on the Aosta-Pre Saint Didier track that are conventionally called DM061, DM068, DM082. A mean value of the kinematic friction coefficient equal to $\mu_c = 0.28$ has been chosen (typical of the most

frequent operating conditions). To obtain as output a single average wheel profile that could be effectively compared with the profile extracted from the numerical simulation and to reduce the measurement errors, the experimental data have been properly processed mediating on all the vehicle wheels (see Tab. 3) [7]. As it can be seen, the flange height FH remains approximately constant because of the low mileage traveled by the vehicles, while the flange thickness FT and the flange steepness QR decrease almost linearly and highlight, according to the characteristics of the track, the wear concentration in the wheel flange. Concerning the rail wear, the QM quota evolution is compared with a criterion present in literature (based on the total tonnage burden on the track) [9]. Particularly a proportionality relationship between tonnage and wear holds: a rail wear of $1\ mm$ on the rail head height every $100Mt$ (millions of tons) of accumulated tonnage.

5.2 The Statistical Approach

The present section is an overview on the procedure used in deriving a significant statistical track description, an essential task to make possible and rationalize the approach and the simulation work on a complex railway line. In the present work the statistical approach has been exploited to draw up a virtual track of the Aosta-Pre Saint Didier line (further details can be found in literature [7]). The basic idea is to substitute the simulation on the whole track with an equivalent set of simulations on short curved tracks (in this research activity the curved tracks length is equal to $l_{ct} = 200m$). More precisely, the curve tracks are obtained dividing the whole track in n_{class} curve radius intervals $[R_{min} - R_{max}]$; each of these is furthermore divided in n_{class} superelevation subclasses $[h_{min} - h_{max}]$ (see Tab. 2). For each radius class, a representative radius R_c is calculated as a weighted average on all the curve radii, using the length of the curve as weighting factor. Similarly for each superelevation subclass the correspondent representative superelevation H is chosen as a weighted average on all the curve superelevation, using the length of curve as a weighting factor. For each representative curve a speed value V is chosen as the minimum value between the maximum speed allowable in curve (equal to $V_{max} = 60$ km/h and depending on the radius, the superelevation and the vehicle characteristics) and the speed $\tilde{V}$ calculated by imposing a non-compensated acceleration $a_{nc}^{lim} = 0.8\,\mathrm{m/s^2}$ [9][5]; for the straight class the speed value, obtained from the track data, is equal to 130 km/h. Finally a weighting factor p_k, calculated as explained in paragraph 4.3, is introduced for each subclass to take into account the frequency of a certain matching radius-superelevation in the track and to diversify the wear contributions of the different curves. By way of example in Tab. 2 is shown the data of the statistical analysis with $n_{class} = 7$.

6 Results

In this section the simulation campaign carried out to study the wheel and rail wear evolution will be described. Then the complete track results will be compared with the experimental data provided by Trenitalia and RFI and the comparison between the complete track results and the statistical analysis ones (with class number $n_{class} = 10$) will be performed. Finally the sensibility analysis of the statistical approach with respect to the n_{class} parameter will be presented.

6.1 Simulation Strategy

The wheel and rail wear evolutions evolve according to different time scales and a fully simulation of such events would require a too heavy computational effort. For this reason the following specific algorithm has been adopted for updating the profiles (more details can be found in literature [7]):

1) to have a good compromise between calculation times and result accuracy a suitable number of discrete steps both for the wheel and for the rail steps have been chosen, $n_{sw} = 20$ and $n_{sr} = 5$:

a) consequently the wheel wear threshold D_{step}^{w} (see section 4.3) has been fixed equal to $0.2\ mm$;

b) the value of the rail wear threshold D_{step}^{r} (see section 4.3) has been set equal to $0.8\ mm$ to obtain an appreciable rail wear during the simulations.

2) the wear evolutions on wheel and rail have been decoupled because of the different scales of magnitude:

a) while the wheel wear evolves, the rail is supposed to be constant: in fact, in the considered time scale, the rail wear variation is negligible;

b) the time scale characteristic of the rail wear evolution, much greater than the wheel wear evolution one, causes the same probability that each discrete rail profile comes in contact with each possible wheel profile. For this reason, for each rail profile, the whole wheel wear evolution (from the original profile to the final profile) has been simulated.

Initially the wheel (starting from the unworn profile w_0^0) evolves on the unworn rail profile r_0 producing the discrete wheel profiles $w_0^0, w_1^0, ..., w_{n_{sw}}^0$ (step $p_{1,1}$). Then the virtual rail profiles $r_1^{(i+1)}$, obtained by means of the simulations (w_i^0, r_0), are arithmetically averaged so as to get the update rail profile r_1 (step $p_{1,2}$). This procedure can be repeated n_{sr} times in order to perform all the rail discrete steps (up to the step $p_{n_{sr},2}$).

Table 2: Data of the curvilinear tracks of the statistical analysis with $n_{class} = 7$.

R_{min} (m)	R_{max} (m)	Superelevation $h_{min} - h_{max}$ (mm)	R_c (m)	H (mm)	V (km/h)	p_k %
150	175	0 - 19	-			
		20 - 39	-			
		40 - 59	-			
		60 - 79	-			
		80 - 99	-			
		100 - 119	162	110	57	0.93
		120 - 140	162	131	60	1.30
175	209	0 - 19	-			
		20 - 39	-			
		40 - 59	-			
		60 - 79	-			
		80 - 99	195	90	60	7.09
		100 - 119	195	103	60	7.42
		120 - 140	195	126	60	5.48
209	259	0 - 19	-			
		20 - 39	-			
		40 - 59	-			
		60 - 79	237	70	60	0.87
		80 - 99	237	83	60	8.76
		100 - 119	237	109	60	4.63
		120 - 140	237	120	60	0.47
259	342	0 - 19	-			
		20 - 39	-			
		40 - 59	293	50	60	0.28
		60 - 79	293	65	60	3.05
		80 - 99	293	83	60	0.90
		100 - 119	293	100	60	0.31
		120 - 140	-			
342	503	0 - 19	-			
		20 - 39	-			
		40 - 59	376	49	60	1.13
		60 - 79	376	62	60	1.26
		80 - 99	-			
		100 - 119	-			
		120 - 140	-			
503	948	0 - 19	-			
		20 - 39	774	24	60	1.73
		40 - 59	774	40	60	0.42
		60 - 79	-			
		80 - 99	-			
		100 - 119	-			
		120 - 140	-			
948	8400	0 - 19	3572	5	60	2.40
		20 - 39	3572	20	60	0.91
		40 - 59	-			
		60 - 79	-			
		80 - 99	-			
		100 - 119	-			
		120 - 140	-			
8400	∞	0	∞	0	130	50.65

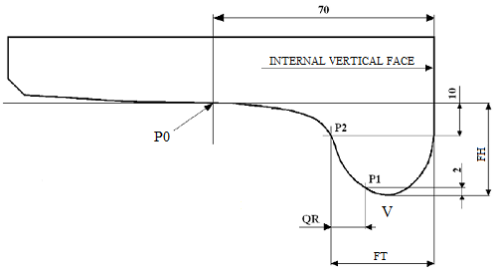

Figure 4: Definition of the wheel wear control parameters.

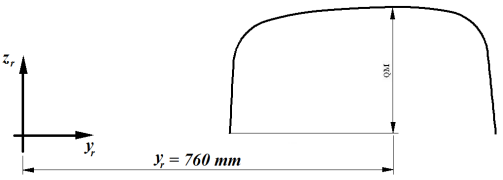

Figure 5: Definition of rail wear control parameter.

Table 3: Experimental processed data.

Vehicle	Distance traveled (km)	FH (mm)	FT (mm)	QR (mm)
DM061	0	28.0	32.5	10.8
	1426	28.2	31.5	9.8
	2001	28.1	30.8	9.1
	2575	28.0	30.2	8.6
DM068	0	28.0	32.5	10.8
	1050	28.0	31.8	10.0
	2253	28.0	30.2	8.5
	2576	28.0	30.0	8.4
DM082	0	28.0	32.5	10.8
	852	28.0	32.3	10.6
	1800	28.0	31.3	9.6
	2802	28.0	30.3	8.7
	3537	27.6	30.0	8.3

6.2 Complete Aosta-Pre Saint Didier Railway Line Results

In this paragraph the results obtained studying the whole Aosta-Pre Saint Didier line will be presented and compared with the experimental data.

6.2.1 Evolution of Wear Control Parameters

The progress of FT dimension, for the n_{sr} discrete step of the rail, is shown in Fig. 6 as a function of the mileage; as it can be seen, the decrease of the dimension is almost linear with the traveled distance except in the first phases, where the profiles are still not conformal enough. The FH quota progress is represented in Fig. 7 and shows that, due to the high sharpness of the considered track and to the few kilometers traveled, the wheel wear is mainly localized on the flange rather than on the tread; therefore the flange height remains near constant in agreement with experimental data (see Tab. 3). The QR trend is shown in Fig. 8: also the flange steepness decreases almost linearly except in the first phases, leading to an increase of the conicity of the flange. Finally the evolution of the wheel control parameters remains qualitatively similar as the rail wear raises, with a slight increase of all the quotas that indicates a shift of the material removed towards the wheel tread, because of the more and more conformal contact (see also Tab. 4, 5). The QM evolution for the analysis of the rail wear is presented in Fig. 9 and shows the almost linear dependence between the rail wear and the total tonnage burden on the track. The amount of removed material on the rail head, equal to $2.97\ mm$, is in agreement with the criterion present in literature [9] ($1\ mm$ on the rail head height every $100\ Mt$ of accumulated tonnage); the total vehicle number $N_{tot} = 2957850$ evolving on the track during the whole simulation procedure corresponds to a tonnage of $M_{tot} = N_{tot} * M_v = 310\ Mt$ (the vehicle mass is $M_v = 104700$ kg (see Tab. 1)) (see Tab. 6, 7).

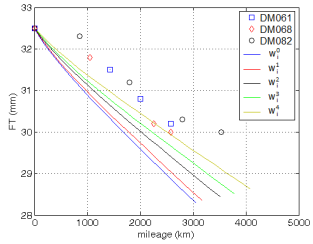

Figure 6: Complete track: FT progress.

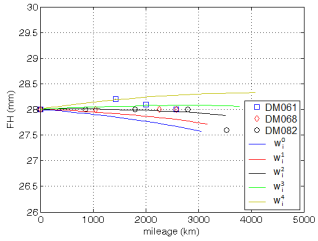

Figure 7: Complete track: FH progress.

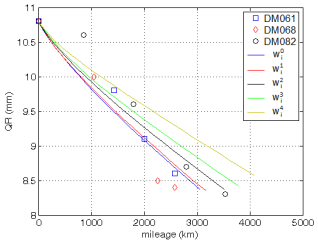

Figure 8: Complete track: QR progress.

6.2.2 *Evolution of the Wheel and Rail Profile*

The wear evolution on the wheel profiles evolving on different rail steps is presented in the Fig. 10, 11 (for reasons of brevity only the profiles evolution related to the first and the last rail steps are represented). As stated previously, the wheel profile evolution is described by means of $n_{sw} = 20$ steps and the threshold on the removed material for each step D^w_{step} has been chosen equal to $0.2\ mm$. The figures show the main localization of the material removed on the wheel flange due to the quite sharp curves that characterize the Aosta-Pre Saint Didier line. In Fig. 12 the evolution of the rail profile is shown, described by means of $n_{sr} = 5$ discrete step and with the threshold on the removed material for each step D^r_{step} equal to $0.8\ mm$.

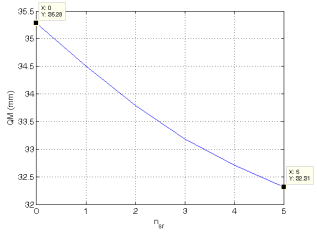

Figure 9: Complete track: QM progress.

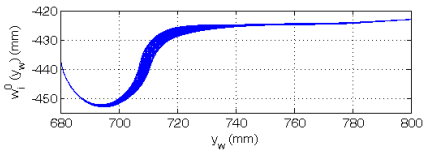

Figure 10: Complete track: w_i^0 evolution.

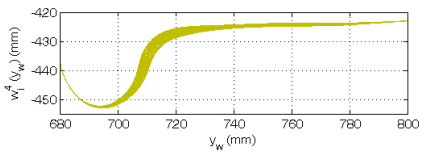

Figure 11: Complete track: w_i^4 evolution.

6.3 Statistical Analysis Results

In this paragraph the results obtained with the statistical analysis approach will be presented. For this purpose a suitable value of the n_{class} parameter have to be supposed. For the Aosta-Pre Saint Didier line the value $n_{class} = 10$, as it will be shown in the following, represents a good compromise among track description, result accuracy and computational effort; in fact a n_{class} too high would increase the result accuracy but would increase the computational time too and would lead to a high number of curve classes quite difficult to be statistically treated.

6.3.1 *Evolution of Wear Control Parameters*

The Figures 13-15 present the evolution of the wear control parameters. It can be seen the same qualitatively trend obtained with the complex railway approach both concerning the conformity considerations and the localization of the worn material on the wheel flange (see also Tab. 4, 5). QM progress lead to a reduction of the rail head height of $3.28\ mm$ in agreement with the criterion present in literature ($1\ mm$ on the rail head height every $100\ Mt$ of accumulated tonnage); in fact the total vehicle number $N_{tot} = 3076200$ evolving on the curved track of the statistical description during the whole simulation corresponds to a tonnage of $M_{tot} = N_{tot} * M_v = 322\ Mt$ (see Tab. 6, 7).

6.3.2 *Evolution of the Wheel and Rail Profile*

As it can be seen in Fig. 16-17, 18, the evolution of the wheel and rail profiles are qualitatively in agreement with the complete railway approach and the same considerations of section 6.2.2 are valid.

6.4 Comparison between the Complete Railway Line and the Statistical Analysis

In this section a quantitatively comparison between the results obtained with the complete railway line and the statistical approach with $n_{class} = 10$ will be carried out. In Tab. 4 the final values of the wheel reference dimensions for all the

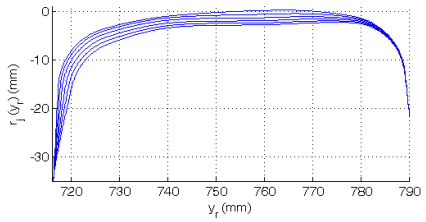

Figure 12: Complete track: rail evolution.

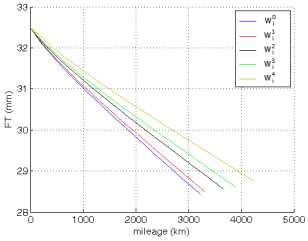

Figure 13: Statistical approach: FT progress.

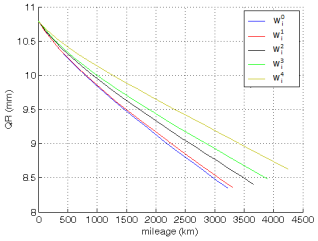

Figure 14: Statistical approach: QR progress.

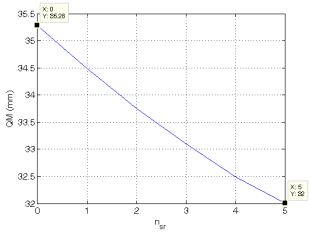

Figure 15: Statistical approach: QM progress.

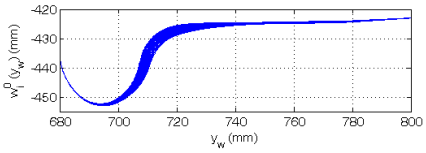

Figure 16: Statistical approach: w_i^0 evolution.

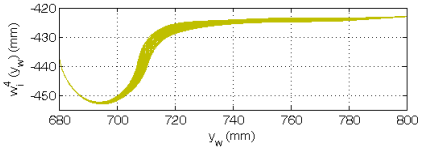

Figure 17: Statistical approach: w_i^4 evolution.

n_{sr} rail step are presented. The increase of the flange height as the rail profile is more and more worn, together with the increase of the flange thickness, indicates a shift of the material removed towards the wheel tread due to the variations of the contact conditions as explained in previous sections. The reference dimension comparison shows a good consistency between the two investigate approaches with a maximum error equal to $e = 1.0\%$.

Table 4: Evolution of the wheel quotas.

	Complete Railway	**Statistical Description** $n_{class} = 10$	
	FH (mm)	FH (mm)	e (%)
km_{tot}^0	27.57	27.86	1.0
km_{tot}^1	27.73	27.98	0.9
km_{tot}^2	27.89	28.12	0.8
km_{tot}^3	28.07	28.27	0.7
km_{tot}^4	28.33	28.60	1.0
	FT (mm)	FT (mm)	e (%)
km_{tot}^0	28.30	28.43	0.5
km_{tot}^1	28.36	28.50	0.5
km_{tot}^2	28.44	28.56	0.4
km_{tot}^3	28.52	28.62	0.4
km_{tot}^4	28.63	28.75	0.4
	QR (mm)	QR (mm)	e (%)
km_{tot}^0	8.38	8.35	0.4
km_{tot}^1	8.35	8.36	0.1
km_{tot}^2	8.37	8.41	0.5
km_{tot}^3	8.43	8.48	0.6
km_{tot}^4	8.57	8.63	0.7

Table 5: Evolution of the total mileage km_{tot}.

	Complete Railway	**Statistical Description** $n_{class} = 10$	
	km_{tot} (km)	km_{tot} (km)	e (%)
km_{tot}^0	3047	3219	5.6
km_{tot}^1	3163	3306	4.5
km_{tot}^2	3515	3659	4.1
km_{tot}^3	3772	3893	3.2
km_{tot}^4	4080	4244	4.0

Table 6: Evolution of the QM quota.

Complete Railway	**Statistical Description** $n_{class} = 10$	
QM (mm)	QM (mm)	e (%)
32.31	32.00	0.6

Table 7: Total vehicle number N_{tot}.

	Complete Railway	**Statistical Description** $n_{class} = 10$	e (%)
N_{tot}	2957850	3076200	4.0

The Tab. 5 displays the evolution of the total mileage km_{tot} as a function of the rail step n_{sr} and shows a good consistency between the two considered procedures: the increase of the mileage traveled by the vehicle as the rail profile is more and more worn indicates a decrease of the wear rate explained by a better conformity between wheel and rail surfaces. In the Tab. 6-7 the comparison of the parameters QM and N_{tot} needed to evaluate the rail wear is shown.

6.5 Sensibility Analysis of the Statistical Approach

In this paragraph a sensibility analysis of the statistical approach with respect to the class number n_{class}, i.e. the most important parameter of the track discretization, will be presented. The variation range studied is $n_{class} = 4 \div 10$. By analyzing the data relative to the wheel presented in Tab. 8, for each value of n_{class} investigated, the trend of the wheel

parameters shows an increase both of the wheel flange dimensions in according to the variation of the contact conditions explained in the previous sections (see 6.2-6.4). Analogously the km_{tot} evolution trend is the same for each of the statistical analysis considered, and also the mileage increases as the rail wear increases indicating the more and more conformal contact between wheel and rail surfaces. The error e presented in Tab. 8 is referred to the complete railway approach and shows less and less consistency between the results of the whole railway approach and the statistical analysis as the n_{class} parameter decreases: in particular small n_{class} values corresponding to a rough discretization of the track, lead to an important underestimation of the removed material highlighted by the increasing mileage traveled. The less accuracy of the model and the underestimation of the worn material as the track description is more and more rough is found also by analyzing the rail control parameter and the number of the train evolving on the track (see Tab. 9).

Table 8: Evolution of the wheel control parameters (quotas and km_{tot}).

Statistical Description		FH (mm)	e (%)	FT (mm)	e (%)	QR (mm)	e (%)	km_{tot} (km)	e (%)
$n_{class} = 4$	km_{tot}^0	26.99	2.1	28.02	1.0	8.29	1.0	3775	23.9
	km_{tot}^1	27.12	2.2	28.16	0.7	8.25	1.2	3967	25.4
	km_{tot}^2	27.26	2.3	28.19	0.9	8.28	1.1	4267	21.4
	km_{tot}^3	27.49	2.1	28.26	0.9	8.35	1.0	4521	19.9
	km_{tot}^4	27.71	2.2	28.35	1.0	8.47	1.2	4793	17.5
$n_{class} = 5$	km_{tot}^0	27.02	2.0	28.03	1.0	8.31	0.9	3713	21.9
	km_{tot}^1	27.16	2.0	28.16	0.7	8.27	0.9	3877	22.6
	km_{tot}^2	27.31	2.1	28.20	0.9	8.29	1.0	4129	17.5
	km_{tot}^3	27.54	1.9	28.27	0.9	8.35	0.9	4397	16.6
	km_{tot}^4	27.75	2.0	28.36	0.9	8.48	1.1	4688	14.9
$n_{class} = 6$	km_{tot}^0	27.08	1.7	28.06	0.8	8.31	0.8	3620	18.8
	km_{tot}^1	27.24	1.7	28.18	0.6	8.28	0.9	3743	18.5
	km_{tot}^2	27.40	1.8	28.23	0.7	8.29	0.9	4038	14.9
	km_{tot}^3	27.62	1.6	28.31	0.8	8.36	0.9	4237	12.3
	km_{tot}^4	27.83	1.8	28.40	0.8	8.48	1.1	4569	12.0
$n_{class} = 7$	km_{tot}^0	27.11	1.7	28.09	0.7	8.31	0.8	3535	16.0
	km_{tot}^1	27.26	1.7	28.19	0.6	8.29	0.8	3676	16.2
	km_{tot}^2	27.43	1.7	28.25	0.7	8.30	0.9	3984	13.3
	km_{tot}^3	27.65	1.5	28.33	0.6	8.36	0.8	4172	10.6
	km_{tot}^4	27.85	1.7	28.42	0.7	8.48	1.0	4503	10.4
$n_{class} = 8$	km_{tot}^0	27.14	1.6	28.10	0.7	8.33	0.6	3431	12.6
	km_{tot}^1	27.30	1.5	28.19	0.6	8.30	0.5	3529	11.6
	km_{tot}^2	27.47	1.5	28.26	0.6	8.31	0.7	3903	11.0
	km_{tot}^3	27.69	1.3	28.35	0.6	8.37	0.8	4092	8.5
	km_{tot}^4	27.90	1.5	28.44	0.7	8.49	0.9	4445	8.9
$n_{class} = 9$	km_{tot}^0	27.20	1.3	28.13	0.6	8.33	0.6	3308	8.6
	km_{tot}^1	27.37	1.3	28.20	0.6	8.32	0.4	3397	7.4
	km_{tot}^2	27.55	1.2	28.28	0.5	8.31	0.6	3777	7.4
	km_{tot}^3	27.77	1.1	28.38	0.5	8.37	0.7	4011	6.4
	km_{tot}^4	27.97	1.3	28.47	0.6	8.50	0.8	4343	6.4
$n_{class} = 10$	km_{tot}^0	27.86	1.0	28.43	0.5	8.35	0.4	3219	5.6
	km_{tot}^1	27.98	0.9	28.50	0.5	8.36	0.1	3306	4.5
	km_{tot}^2	28.12	0.8	28.56	0.4	8.41	0.5	3659	4.1
	km_{tot}^3	28.27	0.7	28.62	0.4	8.48	0.6	3893	3.2
	km_{tot}^4	28.60	1.0	28.75	0.4	8.63	0.7	4244	4.0

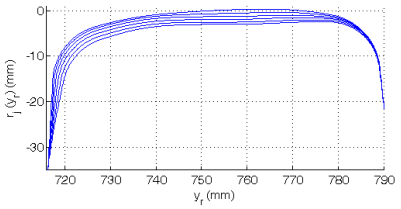

Figure 18: Statistical approach: rail evolution.

Table 9: Rail control parameters evolution (QM quota and N_{tot}).

Statistical Description	QM (mm)	e (%)	N_{tot}	e (%)
$n_{class} = 4$	31.58	2.3	3797900	28.4
$n_{class} = 5$	31.63	2.1	3641100	23.1
$n_{class} = 6$	31.69	1.9	3543500	19.8
$n_{class} = 7$	31.75	1.7	3398600	14.9
$n_{class} = 8$	31.83	1.5	3309800	11.9
$n_{class} = 9$	31.86	1.4	3188600	7.8
$n_{class} = 10$	32.00	1.0	3076200	4.0

Table 10: Processor and integrator data.

Processor	INTEL Xeon CPU X5560 2.80 GHz 24GB RAM	
Integrator	Type	ODE5
	Alghoritm	Dormand-Prince
	Order	5
	Step type	fixed
	Stepsize	10^{-4} s

6.6 Computational Effort Comparison

In this section the comparison between the computational load required by the different approaches considered in this work, i.e. the complete railway line and all the analyzed statistical track descriptions ($n_{class} = 4 \div 10$), will be performed. The characteristics of the processor and the integrator parameters used for the dynamical simulations are briefly reported in Tab. 10. The mean computational times relative to each discrete step of the whole model loop are schematically summarized in Tab. 11 (t_{wt}, t_{rt} are the total simulation time for wheel and rail respectively, t_{wd} and t_{rd} the dynamical simulation times and t_{ww}, t_{rw} the wear simulation times).

The huge computational effort that affects the complete railway line simulation, makes this approach hardly feasible to the wear evolution studies typical of the railway field. On the contrary the statistical track description (see the Tab. 8, 9 and 11) shows a high saving of computational load and at the same time a not excessive loss of model accuracy; in particular, with a number of curve classes $n_{class} = 10$, wear evaluation results are qualitatively and quantitatively in agreement with the complete line approach (a maximum error $e \simeq 5\%$ on the mileage traveled by the vehicle has been found). In conclusion the innovative wear model developed for the study of complex railway networks using a statistical track description approach is capable of simulating the wear evolution both on the wheel and on the rail surfaces with reasonable computational time and leads to a good result consistency if compared to the considered experimental data.

Table 11: Computational time.

Railway approach		Computational time						
		Wheel wear evaluation			Rail wear evaluation			Total simulation time
		t_{wd}	t_{ww}	t_{wt}	t_{rd}	t_{rw}	t_{rt}	t_T
Complete track		4d 12min	1d 38min	5d 50min	3dd 12h	1d 8h 40min	4dd 20h 40min	24dd 7h 20min
Statistical analysis	$n_{class} = 4$	8min	4min	12min	2h 40min	1h 20min	4h	20h
	$n_{class} = 5$	11min	4min	15min	3h 40min	1h 20min	5h	1d 1h
	$n_{class} = 6$	13min	6min	19min	4h 20min	2h	6h 20min	1d 7h 40min
	$n_{class} = 7$	15min	7min	22min	5h	2h 20min	7h 20min	1d 12h 40min
	$n_{class} = 8$	18min	7min	25min	6h	2h 20min	8h 20min	1d 16h 40min
	$n_{class} = 9$	21min	9min	30min	7h	3h	10h	2dd 2h
	$n_{class} = 10$	24min	10min	34min	8h	3h 20min	11h 20min	2dd 8h 40min

7 Conclusions

In this work the Authors presented a complete model for the wheel and rail wear prediction in railway applications specifically developed (in the collaboration with Trenitalia S.p.A and Rete Ferroviaria Italiana (RFI)) for complex railway networks where the exhaustive analysis on the complete line is not feasible because of the computational load required. The most innovative aspect of the model is the track statistical approach based on the replacement of the complete railway line with a statistically equivalent set of representative curved tracks (classified by radius, superelevation and traveling speed). The whole model has been validated on a critical scenario in terms of wear in Italian railways: the ALSTOM *DMU Aln 501 Minuetto* circulating on the Aosta-Pre Saint Didier railway line. Particularly the new model results have been compared both with the complete railway network ones and with the experimental data provided by Trenitalia. If the track discretization is accurate enough, the developed model turned out to be quite in agreement both with the experimental data and with the complete railway network model, and the evolution of all the profile characteristic dimensions described in a satisfying way the wear progress both on the wheel and on the rail. As regard to the track description, the statistical analysis turned out to be a good approach with a significant saving of computational time despite a very slight loss of the result accuracy if compared to the complete railway network model.

Future developments will be based on further validations of the whole model through new experimental data always provided by TI and on a better investigation of the statistical approach. In this way further improvements of the statistical analysis (mainly related to tracking and braking actions, impulsive events such as the track switches and weather conditions) will be possible.

References

[1] F. Braghin, R. Lewis, R. S. Dwyer-Joyce, and S. Bruni. A mathematical model to predict railway wheel profile evolution due to wear. *Wear*, 261:1253–1264, 2006.

[2] Joao Pombo, Jorge Ambrosio, Manuel Pereira, Roger Lewis, Rob Dwyer-Joyce, Caterina Ariaudo, and Naim Kuka. Development of a wear prediction tool for steel railway wheels using three alternative wear functions. *Wear*, 20:327–358, 2011.

[3] E. Meli, S. Falomi, M. Malvezzi, and A. Rindi. Determination of wheel - rail contact points with semianalytic methods. *Multibody System Dynamic*, 20:327–358, 2008.

[4] J. J. Kalker. *Three-dimensional Elastic Bodies in Rolling Contact*. Kluwer Academic Publishers, Dordrecht, Netherlands, 1990.

[5] P. Toni. Ottimizzazione dei profili delle ruote su binario con posa 1/20. Technical report, Trenitalia S.p.A., 2010.

[6] S. Iwnicki. *The Manchester Benchmarks for Rail Vehicle Simulators*. Swets and Zeitlinger, Lisse, Netherland, 1999, 2008.

[7] M. Ignesti, M. Malvezzi, L. Marini, E. Meli, and A. Rindi. Development of a wear model for the prediction of wheel and rail profile evolution in railway systems. *Wear*, 284-285:1–17, 2012.

[8] EN 15313: Railway applications — In-service wheelset operation requirements — In-service and off-vehicle wheelset maintenance, 2010.

[9] C. Esveld. *Modern Railway Track*. Delft University of Technology, Delft, Netherland, 2001, 1985.